Do Sodium Oxofluoroaluminates Exist at Room Temperature?

Marián Kucharík,[a] Miroslav Boča,*[a,c] Catherine Bessada,[b] and Hartmut Fuess[c]

Keywords: Oxofluoroaluminate species / Alumina / Cryolite

Alumina dissolution in cryolite melts is currently associated with the formation of oxofluorospecies. Mixtures of Na_3AlF_6 and Al_2O_3 were heated under different conditions of temperature, time and atmosphere. The existence of oxofluorospecies in solidified samples at room temperature was investigated by X-ray diffraction, IR and Magic Angle Spinning NMR spectroscopy. The formation of β-alumina ($NaAl_{11}O_{17}$) was detected depending on the heating conditions, but no oxofluoroaluminate species were found.

Introduction

During 50 years of structural investigation on cryolite–alumina melts, numerous suggestions on the nature of the possible oxygen-containing species in the melt have been presented.[1] Førland and Ratkje[2] from cryoscopic measurements on the sodium fluoride-rich side in the reciprocal salt system $NaF–AlF_3–Na_2O–Al_2O_3$ suggested the preferred formation of the $Al_2OF_x^{(4-x)}$ ($x = 5–8$) anion for an ionic ratio of Al^{3+}/O^{2-} greater than five. Based on vapour pressure measurements, Kvande[3] proposed that $Al_2OF_8^{4-}$ is the most important anion for low alumina content in cryolite melts. Sterten[4] developed an ionic structure model for NaF/AlF_3 melts containing alumina. The calculations of anion fractions as a function of the cryolite ratio (*CR*; molar ratio between NaF and AlF_3) suggested that $Al_2OF_6^{2-}$ and $Al_2O_2F_4^{2-}$ are the most frequent species for $1.5 < CR > 3$. For $CR > 5$ the complex anions $Al_2O_2F_4^{2-}$ and $Al_2O_2F_6^{4-}$ were most important. Bache and Ystenes[5] interpreted IR and X-ray diffraction results of quenched mixtures of cryolite and chiolite together with alumina as free of α-Al_2O_3 but consisting of some unspecified oxofluoroaluminates.

The Raman data and thermodynamic measurements of Gilbert et al.[6] and Robert et al.[7] indicate the formation of $Al_2OF_6^{2-}$ or $Al_2OF_8^{4-}$ ions for melts with low Al_2O_3 concentrations. However, at higher Al_2O_3 concentration, $Al_2O_2F_4^{2-}$ anions would be predominant. Daněk et al.[8] directly determined the presence of oxygen on samples from $MF–AlF_3–Al_2O_3$ (M = Li, Na, K) by using a LECO TC–436 Nitrogen/Oxygen analyser. They claim that three anion species are present in $NaF/AlF_3–Al_2O_3$ melts, that is, $Al_2OF_6^{2-}$, $Al_3O_3F_6^{3-}$and $Al_2O_2F_4^{2-}$. At up to 2 mol-% of Al_2O_3 only the $Al_2OF_6^{2-}$ and $Al_3O_3F_6^{3-}$ species are present. At high alumina content, $Al_2O_2F_4^{2-}$ species are abundant. The above assumption was also confirmed by Lacassagne et al.[9] They studied the structure of $NaF/AlF_3–Al_2O_3$ melts by high-temperature NMR spectroscopy for the four nuclei ^{27}Al, ^{23}Na, ^{19}F, and ^{17}O. ^{17}O NMR spectroscopy gave a selective view of the alumina dissolution in molten cryolite, because of its direct signature of the oxofluoride complexes. The variations in the ^{17}O chemical shift were explained by the presence of at least two different oxofluoroaluminate species: $Al_2OF_6^{2-}$ at low alumina content and $Al_2O_2F_4^{2-}$, which becomes the major species for higher amounts of alumina.

If the presence of these oxofluoroaluminate species in the molten state has been demonstrated by spectroscopy, it is difficult to prove their presence in the solidified state. Only Brooker et al.[10] observed Raman spectra with bands that could be assigned to the $Al_2OF_6^{2-}$ anion. Their Raman spectra were obtained from a premelted solid sample containing 5 mol-% Na_2O and 5 mol-% AlF_3 in FLINAK. The bands at 509 cm^{-1} were assigned to the oxide-bridged, totally symmetric stretching mode of $Al_2OF_6^{2-}$. The same bands were observed at 494 cm^{-1} in the molten system with identical composition.

For a better understanding of the spectroscopic signatures of the species formed in the melts, it would be of great interest to succeed in forming stable solid oxofluoroaluminate phases at room temperature.

In order to contribute to the knowledge of oxofluoro–aluminium species, we have studied different solidified mixtures of Na_3AlF_6 and Al_2O_3 by IR spectroscopy, X-ray powder diffraction and multinuclear MAS NMR spec-

---

[a] Institute of Inorganic Chemistry, Slovak Academy of Sciences,
Dúbravská cesta 9, 84536 Bratislava, Slovakia
Fax: +421-(0)2-59410444
E-mail: uachboca@savba.sk
[b] Centre de Recherche sur les Matériaux à Haute Température, CRMHT-CNRS,
1D avenue de la Recherche Scientifique, 45071 Orléans Cedex 2, France
[c] Institute of Materials Science, Darmstadt University of Technology,
Petersenstrasse 23, 64289 Darmstadt, Germany

DOI: 10.1002/ejic.200400814

troscopy. The combination of these different techniques provides a more precise identification of the different phases formed on cooling.

Results and Discussion

X-ray Powder Diffraction and IR Spectra

Heating under Inert Atmosphere

In the X-ray powder diffraction patterns of the samples **1a** and **1b** only the cryolite phase was clearly detected. The presence of crystalline alumina is not evident. The same conclusion can be reached by considering the IR spectra. No reaction products are therefore present in the mixture, as no reaction seems to take place between cryolite and alumina under inert atmosphere at these experimental conditions.

Heating under Air

X-ray powder diffraction patterns of the samples **2a**, **3a** and **4a** are displayed in Figure 1. After heating for 10 and 20 h only cryolite and α–alumina were detected in **2a** and **3a**. The XRD pattern of sample **4a**, after 50 h of heating, clearly corresponds to $NaAl_{11}O_{17}$. In the case of samples **2b**, **2c**, **3b** and **3c**, a mixture of all components was found (cryolite, α-Al_2O_3, NaF and $NaAl_{11}O_{17}$) while only $NaAl_{11}O_{17}$ was detected in **4b** and **4c**.

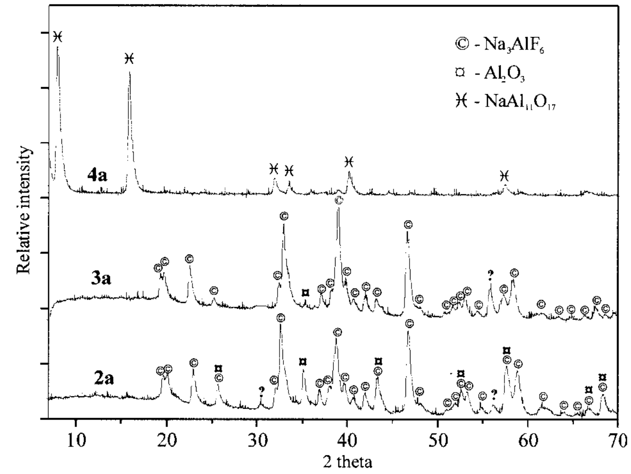

Figure 1. X-ray powder diffraction patterns of the samples **2a**, **3a** and **4a**.

In the IR spectra of all samples (**2b**, **2c**, **3a**, **3b**, **3c**, **4a**, **4b** and **4c**; see Figure 2) cryolite with different concentrations of α–alumina was detected, probably because of the incomplete reaction due to its high concentration. In all samples, except for **2a**, new peaks were detected. The intensities of these new peaks increase with increasing heating time. After 10 and 20 h of heating, peaks at 1135 cm^{-1} and 705 cm^{-1} were observed and after 50 h a peak at 1136 cm^{-1} splits into two peaks at 1148 cm^{-1} and 1121 cm^{-1}. Moreover, two new peaks are also detected at 627 cm^{-1} and at 667 cm^{-1}. The peak at 706 cm^{-1} remains unchanged.[11] These new peaks can be related to the formation of the sodium oxoaluminate $NaAl_{11}O_{17}$. This result will be supported by MAS NMR measurements in the following section.

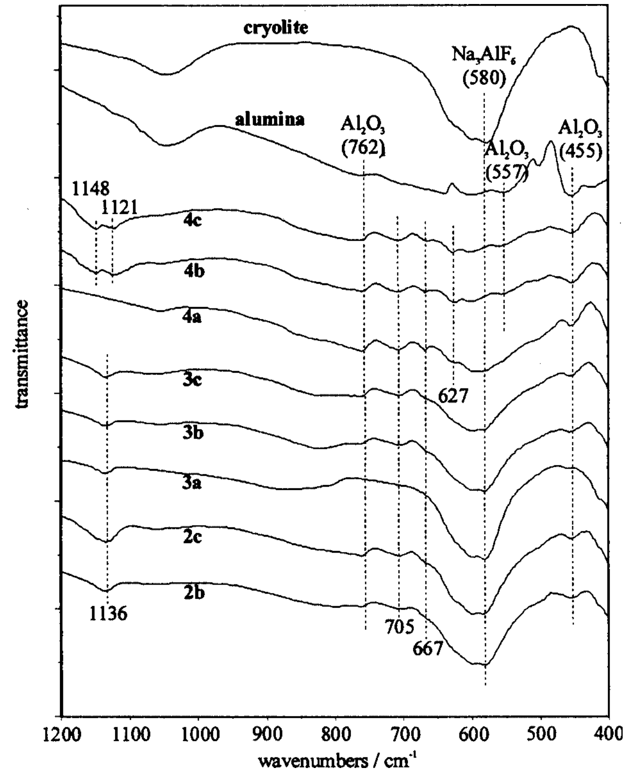

Figure 2. IR spectra of the samples **2b**, **2c**, **3a**, **3b**, **3c**, **4a**, **4b** and **4c**.

Heating in Closed Pt Tubes

The results for this series of experiments (**5a**, **5b**, **5c**, **6a**, **6b**, **6c**, **7a**, **7b**, **7c**, **8** and **9**) are surprisingly identical to those of samples **1a** and **1b**. Crystalline cryolite is detected clearly by both X-ray powder diffraction measurements and by IR spectroscopy while the presence of crystalline alumina is more questionable. No other phases were detected. The only difference can be observed in samples **8** and **9** where α-Al_2O_3 is clearly detected in the X-ray powder diffraction patterns and IR spectra. It means that on spontaneous cooling (samples **8** and **9**) crystalline α-Al_2O_3 can solidify, while for faster cooling (samples **5**–**7**) only crystalline cryolite can be detected without any doubt.

^{27}Al, ^{23}Na and ^{19}F MAS NMR Spectra

^{27}Al MAS NMR Spectra

Aluminium is a quadrupolar nucleus (I = 5/2) and spectra obtained in the solid phase, even at fast MAS conditions, can be very complex.[12] Because of the lines overlapping at 9.4 T, we also report some spectra obtained at higher field (17.6 T) in order to obtain a better resolution. The second order quadrupolar interaction is then minimized and leads to simplified line shapes.

We have reported a comparison of ^{27}Al MAS spectra obtained at 9.4 T for different mixtures with those of the starting materials: cryolite and α-Al_2O_3 (see Figure 3). The ^{27}Al signature of cryolite is very simple and corresponds to a single $\{AlF_6\}$ site, with a chemical shift at ca. 0 ppm, and very low quadrupolar coupling ($\nu_Q \approx 150$ kHz).[13] For α-alumina, one peak is observed at about 14 ppm corresponding to the $\{AlO_6\}$ environment in the solid state at room temperature. For the mixture of 30 mol-% Al_2O_3 in cryolite heated for 20 h at 1010 °C under air (samples **3b** and **3c**) the spectra are rather complex. In addition to the peaks corresponding to different starting constituents of the mixture, that is, cryolite and α-alumina, we can also detect at least two other signals, with broad quadrupolar line shapes identified by their maxima at $\delta \approx 65$ ppm and at $\delta \approx 75$ ppm.[14] By combining the ^{27}Al MAS spectra obtained at 9.4 T and 17.6 T, we tried to model the NMR spectra more precisely and to determine the different contributions (see Table 2). We can propose some quantitative description of the different phases, in agreement with the XRD conclusions. In addition to the cryolite and α-Al_2O_3 signals, we can evidence typical signatures of transition alumina, with one signal at $\delta = 18$ ppm attributed to six-coordinate aluminium, and a signal at $\delta = 65$ ppm for four-coordinate aluminium (see Table 1).

Two contributions can be assigned to the two structurally non-equivalent tetrahedral $\{AlO_4\}$ environments of the $NaAl_{11}O_{17}$ phase. In the structure of $NaAl_{11}O_{17}$ both octahedral $\{AlO_6\}$ and tetrahedral $\{AlO_4\}$ fragments are clearly resolved.[15]

In order to discuss the broad "amorphous" component, ^{19}F/^{27}Al CP MAS coupled with 2D MQ MAS experiments are under progress and will give a more precise view of that complex system.

For the sample **4a**, heated for 50 h, the peak corresponding to alumina remains unchanged and the intensity of the signal of cryolite is rather lowered. Moreover, it was not observed in X-ray powder diffraction patterns, so this confirms its very low contribution. We still detect the very

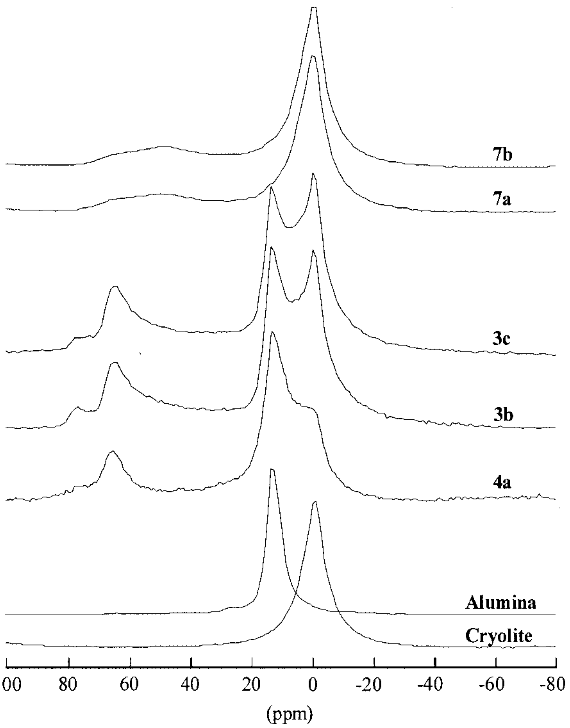

Figure 3. ^{27}Al MAS NMR spectra of the samples **4a**, **3b**, **3c**, **7a** and **7b** in relation with the spectra of the starting materials: cryolite and alumina. The spectra were obtained at 9.4 T with a spinning speed of 32.5 kHz.

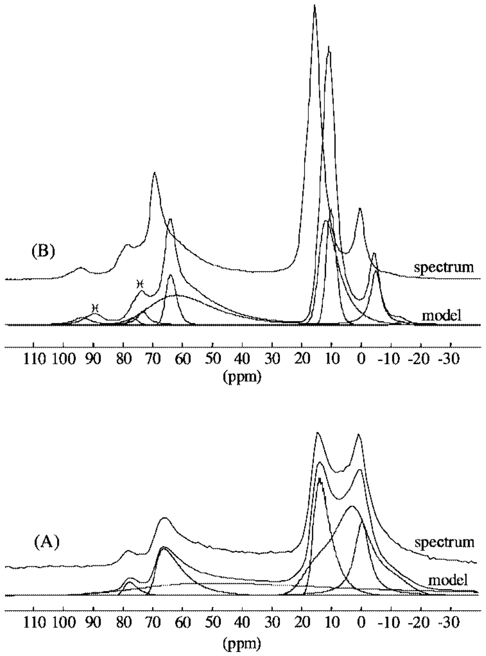

Figure 4. ^{27}Al MAS NMR spectra of the sample **3b** obtained at two different magnetic fields and its decomposition in different contributions.[26] The upper spectrum was obtained at 17.6 T (B) and the lower at 9.4 T (A). The model spectra were computed using the same set of parameters, considering six different sites: three $\{AlO_4\}$, two $\{AlO_6\}$ and one $\{AlF_6\}$. The NMR parameters deduced from the fit are reported in Table 2. The asterisks (*) represent spinning side bands.

Table 1. NMR parameters deduced from the fit[26] of the experimental ^{27}Al MAS spectrum of the sample **3b**. The same set of parameters was used for the fits at 9.4 T and 17.6 T. δ_{iso} is the isotropic chemical shift; ν_Q is the quadrupolar frequency; η is the asymmetry parameter; I is the relative intensity.

Sites	AlO_4 sites			AlO_6 sites		AlF_6
δ_{iso} (ppm)	78.5 ± 1.5	68.5 ± 1	77 ± 3	19 ± 0.5	15.5 ± 0.5	-0.5 ± 0.5
ν_Q (kHz)	300 ± 50	480 ± 40	1300 ± 150	700 ± 40	360 ± 40	150 ± 20
η	0.6 ± 0.2	0.6 ± 0.2	0.6 ± 0.2	1 ± 0.2	0.6 ± 0.2	0 ± 0.2
I (%)	1 ± 0.5	9 ± 2	32 ± 2	30 ± 4	15 ± 1	13 ± 1

broad contribution at around 75 ppm. From the ^{27}Al chemical shift range reported in oxides and fluorides,[16] this high chemical shift cannot be due to the oxofluoro environment for the aluminium atoms in the solidified samples but to the oxide environment (see Figure 4).

^{19}F MAS NMR Spectra

In the ^{19}F MAS NMR spectra we observed unambiguously the signal for cryolite (–190 ppm) and the signal for NaF (–225 ppm)[9] in the samples **3b**, **3c** and **4a**, in agreement with the X-ray powder diffraction and IR spectroscopy results. In the samples **7a** and **7b** only cryolite is present and no other fluoro-species were observed. The ^{19}F chemical shifts-range, reported by Chupas et al.[17] for octahedral aluminium environments with oxygen and fluorine in the first coordination sphere, lies between –115 and –170 ppm. No such signal is detectable in our ^{19}F MAS spectra.

From these experiments we can state the absence of all fluoro-species except for cryolite (see Figure 5).

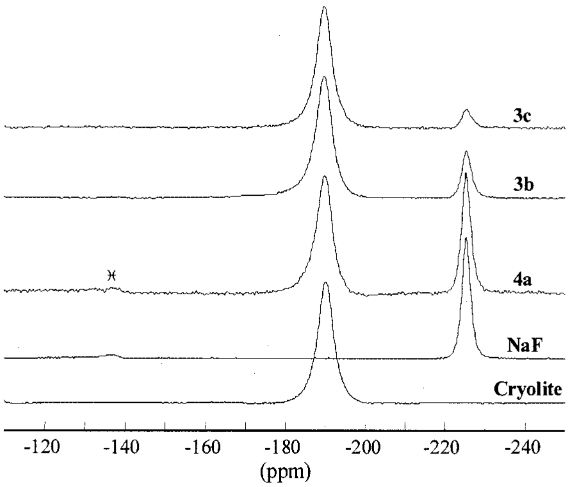

Figure 5. ^{19}F MAS NMR spectra of the samples **4a**, **3b**, **3c**, cryolite and NaF obtained at 9.4 T and at a spinning speed of 32 kHz. The asterisk (*) represents spinning side bands.

^{23}Na MAS NMR Spectra

The signals observed in **3b** and **3c** are superpositions of the cryolite signals ($\delta \approx 1$ ppm and $\delta \approx -11/-14$ ppm) and NaF at $\delta \approx 7$ ppm (see Figure 6).[9] A broad component (clearly visible in the **4a** spectrum) is also observed around –21 ppm. This peak is not easily assigned because of its strong overlap with the other signals, but it can be related to the $NaAl_{11}O_{17}$ phase detected by ^{27}Al NMR spectroscopy. A better resolution could be achieved by a ^{23}Na MQMAS experiment that would provide separation of these different contributions. In the case of samples **7a** and **7b**, again we observed only the signal for cryolite (not reported here).

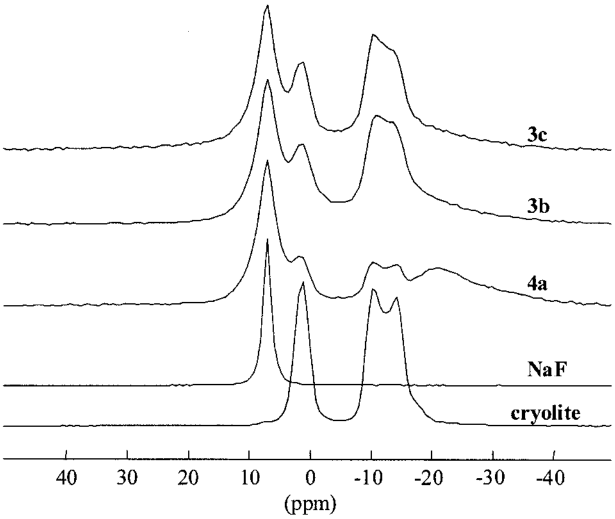

Figure 6. ^{23}Na MAS NMR spectra of the samples **4a**, **3b**, **3c**, cryolite and NaF obtained at 9.4 T and at a spinning speed of 32 kHz.

From different phase diagrams reported for the system Na_3AlF_6–Al_2O_3,[18–20] the eutectic point reported is around 10 wt.-% Al_2O_3 (18.6 mol-%) with an eutectic temperature of 966 °C. Skybakmoen et al.[20] determined the solubility of alumina in molten Na_3AlF_6 by measuring the weight loss of a rotating sinter-corundum disc in the cryolite melt. The results were fitted to [Equation (1)].

$$[Al_2O_3]_{sat} = A\left(\frac{t}{1000}\right)^{B} \qquad (1)$$

where $A = 11.9$, $B = 4.8$ and t is the temperature in °C; the square brackets denote the weight percentage of alumina at saturation (the equation also contains terms for AlF_3, CaF_2, MgF_2 and LiF, which are not included here). According to the above equation, the solubility of alumina in cryolite at 1010 °C is 12.5 wt.-% (22.7 mol-%) Al_2O_3.

In our experiments, we have mainly used a composition of 30 mol-% (17.3 wt.-%) Al_2O_3 in the cryolite melt. At 1010 °C Al_2O_3 is 7.3 mol-% over the solubility limit. During prolonged heating, vapours of $NaAlF_4$ are expected to be formed,[21] as described by [Equation (2)].

$$Na_3AlF_6\ (l) = 2\ NaF\ (l) + NaAlF_4\ (g) \qquad (2)$$

and consequently $NaAlF_4$ can decompose during condensation on the top parts of the apparatus according to [Equation (3)].

$$NaAlF_4\ (g) = 1/5\ Na_5Al_3F_{14}\ (s) + 2/5\ AlF_3\ (s) \qquad (3)$$

In such a case, the system is enriched in NaF. According to the phase diagram of the system Na_6F_6–Al_2F_6–Al_2O_3–Na_6O_3, given by Foster,[22] the α–alumina in excess is transformed into β-alumina. This process can be expressed by [Equation (4)].

$$2\ NaF\ (l) + (3x + 1)/3\ Al_2O_3\ (s, \alpha) = Na_2O{\cdot}xAl_2O_3\ (s) + 2/3\ AlF_3\ (l) \qquad (4)$$

where $x = 11$.

The above explanations are based on an open system. In the closed system, the results could be explained by the following considerations.

In molten cryolite, it is generally accepted that the ions present are Na^+, F^-, AlF_4^-, AlF_5^{2-} and AlF_6^{3-}. Alumina $[(Al_2O_3)_n]$ dissolves and provides the probable anions AlO_2^- and AlO^+ (the presence of other anions such as $Al_{2n+1}O^-_{3n+2}$ or $Al_{2n+1}O^+_{3n+1}$ cannot be excluded) that would give oxofluoro-anions by reacting in the melt. Even if fluoro- and oxo-anions react in the melt to form oxofluoroaluminates, the cooling rate of ca. 1000 °C/min is not high enough to trap them and may lead to the decomposition of oxofluoroaluminates into cryolite and some amorphous alumina phase (sample **7**). If the cooling rate is even slower (spontaneous cooling), there is enough time to form the crystalline phase of α-alumina (samples **8** and **9**). No reaction seems to take place between cryolite and alumina.

In the case of sample **7**, we observed the NMR signal of cryolite, and no signal for alumina. These results coincide rather well with the observations made by other authors who reported only the cryolite phase from X-ray powder patterns of quenched mixtures of alumina and cryolite.[23,24] An attempt to explain the nature of alumina in quenched cryolite–alumina melts was suggested by Foster.[25] He concluded that alumina dissolves in cryolite to produce one or more species, that is, oxoaluminates or oxofluoroaluminates. He was not able to prove or exclude the presence of oxofluoroaluminate species. Thus he stated that they are only stable in the liquid phase or in insufficient amounts in the mixture below the detection limit of the X-ray diffractometer. According to our investigation, we still cannot decide whether oxofluoroaluminates are stable only in melts but we can exclude their presence in the solidified samples.

Conclusions

The results obtained by X-ray powder diffraction, IR and NMR spectroscopy allow us to give some conclusions about the presence of oxofluoroaluminate species in the solidified mixtures of cryolite and alumina.

Heating 30 mol-% alumina in cryolite under air at 1010 °C for 50 h results in an almost complete reaction of the mixture in $NaAl_{11}O_{17}$ and NaF. The existence of oxofluoroaluminate species can be excluded in the solid phase.

Heating of the alumina–cryolite mixture in hermetically closed Pt tubes at 1500 °C or under an inert atmosphere at 1010 °C and subsequent quenching provides some amorphous alumina phases. No decomposition providing NaF was observed and the presence of oxofluoroaluminates in the solid phase can be excluded.

Heating of the alumina–cryolite mixture in hermetically closed Pt tubes at 1500 °C or under an inert atmosphere at 1010 °C and consequent, spontaneous cooling provides crystalline cryolite with a crystalline alumina phase. No decomposition leading to NaF was observed and the presence of oxofluoroaluminates in the solid phase can be further excluded.

Experimental Section

The chemicals used are hand-picked powdered cryolite from Greenland (m. p. 1009–1011 °C) and powdered Al_2O_3 (Merck, p.a.). The powders were treated in a resistance furnace with a Kanthal coil equipped with a vertical alumina tube and a calibrated Pt–Pt/10Rh thermocouple located close to a platinum crucible.

Heating under Inert Atmosphere: A mixture of Na_3AlF_6 and 30 mol-% Al_2O_3 was heated under nitrogen at 1010 °C for 30 h in the Pt crucible covered with a lid. The nitrogen was bubbled through concentrated sulphuric acid in order to remove water traces. The mixture was then quenched by immersing the platinum crucible with the sample into crushed ice, with a cooling rate of ca. 1000 °C/min. Two samples were collected and powdered. Sample **1a** corresponds to the bottom of the crucible while sample **1b** corresponds to the upper part of the crucible, where the sample condensed and "climbed up" during the experiment (see Figure 6).

Heating under Air: Three mixtures of Na_3AlF_6 and 30 mol-% Al_2O_3 were heated under air at 1010 °C for 10 h (**2**), for 20 h (**3**) and for 50 h (**4**) in the Pt crucible covered with the lid. The mixtures were then treated as in the previous experiment. For each experiment, three samples were collected and powdered: from the bottom of the crucible (**2a**, **3a**, **4a**), from the upper part (**2b**, **3b**, **4b**) and from under the lid (**2c**, **3c**, **4c**) (see Figure 7).

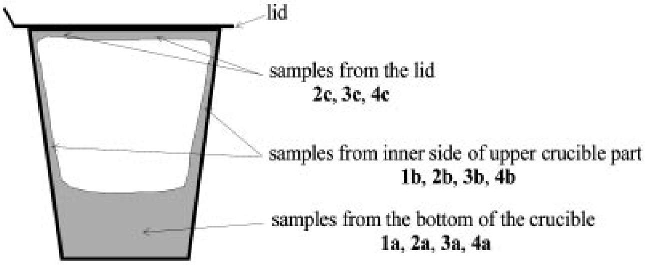

Figure 7. Schematic representation of the position of the investigated samples.

Heating in closed Pt tubes: The mixtures of Na_3AlF_6 and 10 mol-% Al_2O_3 (**5**), 20 mol-% Al_2O_3 (**6**) and 30 mol-% Al_2O_3 (**7**) were heated in the hermetically closed (by welding) Pt tubes at 1500 °C for 15 h and then quenched into ice. The tubes were opened with a saw and the samples collected were powdered. For each composition, three samplings were made from the bottom (**5a**, **6a**, **7a**), the middle (**5b**, **6b**, **7b**) and the top (**5c**, **6c**, **7c**) of the Pt tube.

The mixtures of Na_3AlF_6 and 20 mol-% Al_2O_3, (**8**) and 30 mol-% Al_2O_3, (**9**) were heated in hermetically sealed Pt tubes at 1500 °C for 5 h and left to cool spontaneously by switching off the furnace, which corresponds to a cooling rate of ca. 1.5 °C/min.

Compositions, heating and cooling conditions for the different samples are summarised in Table 2.

X-ray Diffraction Analysis: was carried out using the Philips PW1349/30 diffractometer with Cu-K_α radiation. The X-ray powder diffraction patterns were measured at room temperature in the range 7–70 °C (2θ). Identification of the different phases present in each sample was performed according to the PDF-2 International Centre for Diffraction Data database.

Infrared Spectra: were obtained using an FTIR spectrometer Nicolet Magna 750 equipped with a DTGS detector. The samples were analysed as KBr pellets.

Magic Angle Spinning NMR: experiments have been carried out on a Bruker DSX 400 NMR spectrometer (9.4 T) at operating fre-

Table 2. Samples description: composition, heating and cooling conditions.

Experiment no.	mol-% Al_2O_3	Heating temperature (°C)	Heating duration (h)	Atmosphere and crucible	Cooling
1	30	1010	30	N_2, Pt crucible with lid	quenching
2	30	1010	10	air, Pt crucible with lid	quenching
3	30	1010	20	air, Pt crucible with lid	quenching
4	30	1010	50	air, Pt crucible with lid	quenching
5	10	1500	15	Pt crucible hermetically closed	quenching
6	20	1500	15	Pt crucible hermetically closed	quenching
7	30	1500	15	Pt crucible hermetically closed	quenching
8	20	1500	5	Pt crucible hermetically closed	slow cooling
9	30	1500	5	Pt crucible hermetically closed	slow cooling

quencies of 104.2 MHz for ^{27}Al, 105.8 MHz for ^{23}Na and 376.3 MHz for ^{19}F. ^{27}Al, ^{23}Na and ^{19}F chemical shifts are referenced to 1 M aqueous solutions of $Al(NO_3)_3$, NaCl and $CFCl_3$, respectively, at room temperature.

^{27}Al and ^{23}Na have nuclear spins of 5/2 and 3/2, respectively, and are thus quadrupolar. In solid state MAS spectra, even in high resolution conditions, line broadening and shifts caused by the second order quadrupolar effect can lead to important overlap of lines, therefore, separation of different peaks becomes difficult and sometimes inaccurate. These quadrupolar effects depend on the quadrupolar interactions and the external magnetic field strength. In order to better understand the ^{27}Al MAS spectra obtained at 9.4 T, we have performed the same experiments at 17.6 T on a Bruker Avance 750 spectrometer. The use of a very high field gives better separation of the different lines and allows us to assign each contribution to the different phases in the sample.

The NMR spectra were acquired using high- and very high-speed Bruker MAS probes with rotors of 4 and 2.5 mm in diameter, for spinning rates of 15 and 32 kHz, respectively. The NMR spectra were fitted using a modified version of the Bruker Winfit program.[26] ^{19}F, ^{27}Al, and ^{23}Na MAS spectra were typically acquired with short pulses of 0.5 μs, recycle delay of 2 s and 1 s, respectively, and each spectrum required approximately 128 acquisitions for fluorine and between 6000 and 12000 scans for ^{27}Al and ^{23}Na.

Acknowledgments

This work was financially supported by the Scientific Grant Agency of the Ministry of Education of the Slovak Republic and the Slovak Academy of Sciences (No. 2/1032/21 and No. 2/4071/04), by the Alexander von Humboldt Foundation and by the EEC ARI contract HPRI-CT-1999–00042.

---

[1] K. Grjotheim, C. Krohn, M. Malinovský, K. Matiašovský, J. Thonstad, *Aluminum Electrolysis. Fundamentals of the Hall – Heroult Process*, 2nd ed., Aluminium Verlag GmBH, Düsseldorf, **1982**.
[2] T. Førland, S. K. Ratkje, *Acta Chem. Scand.* **1973**, *27*, 1883–1890.
[3] H. Kvande, *Electrochim. Acta* **1980**, *25*, 273–240.
[4] A. Sterten, *Electrochim. Acta* **1980**, *25*, 1673–1677.
[5] Ø. Bache, M. Ystenes, *Acta Chem. Scand.* **1989**, *43*, 97–98.
[6] B. Gilbert, E. Robert, E. Tixhon, J. E. Olsen, T. Østvold, *Light Metals* **1995**, 181–194.
[7] E. Robert, J. E. Olsen, V. Daněk, E. Tixhon, T. Østvold, B. Gilbert, *J. Phys. Chem. Sect. B* **1997**, *101*, 9447–9457.
[8] V. Daněk, Ø. T. Gustavsen, T. Østvold, *Can. Metall. Q.* **2000**, *39*, 153–162.
[9] V. Lacassagne, C. Bessada, P. Florian, S. Bouvet, B. Ollivier, J. P. Coutures, D. Massiot, *J. Phys. Chem. Sect. B* **2002**, *106*, 1862–1868.
[10] M. H. Brooker, R. W. Berg, J. H. Von Barner, N. J. Bjerrum, *Inorg. Chem.* **2000**, *39,* 4725–4730.
[11] We are aware of IR spectra of $NaAl_{11}O_{17}$ only in the FAR region, so a direct comparison with our results is not possible; S. Edvardsson, L. Ojamae, J. O. Thomas, *Phys. Condens. Matter.* **1994**, *6*, 1319–1332.
[12] M. E. Smith, E. R. H. Van Eck, *Progr. NMR Spec.* **1999**, *34*, 159–201.
[13] D. R. Spearing, J. F. Stebbins, I. Farnan, *Phys. Chem. Min.* **1994**, *21*, 373–386.
[14] G. Kunath-Fandrei, T. J. Bastow, J. S. Hall, C. Jäger, M. E. Smith, *J. Phys. Chem.* **1995**, *99*, 15138–15141.
[15] N. J. Zhu, F. Guo, Y. Li, S. X. Shen, L. R. Chen, A. C. Li, *Hua Hsueh Hsueh Pao* **1992**, *50*, 527–532.
[16] C. Bessada, V. Lacassagne, D. Massiot, P. Florian, J. P. Coutures, E. Robert, B. Gilbert, *Z. Naturforsch. Teil A* **1999**, *54*, 162–166.
[17] P. J. Chupas, D. R. Corbin, V. N. M. Rao, J. C. Hanson, C. Grey, *J. Phys. Chem. B* **2003**, *107*, 8327–8336.
[18] J. L. Holm, *Tiddsskr. Kjemi. Bergv., Met.* **1966**, *10*, 165–171.
[19] A. Sterten, I. Maeland, *Acta Chem. Scand.* **1985**, *39*, 241–257.
[20] E. Skybakmoen, A. Solheim, A. Sterten, *Met. Mater. Trans. B.* **1997**, *28B*, 81–86.
[21] M. Bruno, O. Herstad, J. L. Holm, *Acta Chem. Scand.* **1998**, *52*, 1399–1401.
[22] P. A. Foster, Jr., *J. Am. Ceram. Soc.* **1975**, *58,* 288–291.
[23] E. Zintl, W. Morawietz, *Z. Anorg. Allgem. Chem.* **1939**, *240*, 145–149.
[24] H. Ginsberg, A. Bohm, *Z. Electrochem.* **1957**, *61*, 313–320.
[25] P. A. Foster, Jr., *J. Electrochem. Soc.* **1959**,*106,* 971–975.
[26] D. Massiot, F. Fayon, M. Capron, I. King, S. Le Calvé, B. J. O. Alonso, B. Durand Bujoli, Z. Gan, G. Hoatson, *Magn. Res. Chem.* **2002**, *40,* 70–76.

Received: September 29, 2004